Brooks DJ, Tambasco N.

Imaging Synucleinopathies.

***Movement Disorders* 2016, 31(6), 814-829.**

REVIEW

Imaging Synucleinopathies

AQ2 AQ9 David J. Brooks[1,2,3]* and Nicola Tambasco[4]

AQ3 [1]Institute of Clinical Medicine, Aarhus University, Aarhus, Denmark
[2]Imperial College London, London, United Kingdom
[3]Newcastle University, Newcastle, United Kingdom
[4]Azienda Ospedaliera e Universitaria di Perugia, Perugia, Italy

ABSTRACT: In this review the structural and functional imaging changes associated with the synucleinopathies PD, MSA, and dementias associated with Lewy bodies are reviewed. The role of imaging for supporting differential diagnosis, detecting subclinical disease, and following disease progression is discussed and its potential use for monitoring disease progression is debated. © 2016 International Parkinson and Movement Disorder Society

Key Words: Parkinson's; MRI; PET; SPECT; MSA; DLB

In both late-onset, idiopathic Parkinson's disease (PD) and the genetic forms associated with alpha-synuclein (α-Syn) mutations and multiplications or leucine-rich repeat kinase 2 (LRRK2) and glucocerebrosidase (GBA) gene mutations, cell loss occurs in association with abnormal α-Syn aggregation. α-Syn fibrils are found in intraneuronal Lewy inclusion bodies and Lewy neuritis, and this pathology targets the dopamine cells in the SNc and midbrain tegmentum, noradrenergic cells in the locus ceruleus, serotonergic cells in the median raphe, and cholinergic projections from the pedunculopontine nucleus and nucleus basalis. The pathology is first thought to arise in the dorsal motor nucleus of the vagus and olfactory bulbs.[1] It then ascends through the brainstem to limbic and association cortex, and 80% of PD cases will eventually develop dementia (PDD) if they survive 20 years with their disease.[2] When dementia is present before or within 1 year of parkinsonism, the condition is labeled dementia with Lewy bodies (DLB).[3] The distribution of aggregated α-Syn as Lewy bodies (LBs) in DLB and PDD is similar, though there is a higher prevalence of concommitant Alzheimer's pathology in DLB.[4]

MSA is another synucleinopathy associated with parkinsonism, but, unlike PD, early autonomic failure, falls and postural instability, and ataxia are clinical features of this disorder. Its pathology differs from PD and is characterized by argyrophilic cytoplasmic glial inclusions containing aggregated α-Syn and ubiquitin found in central white matter (WM), the SN and the striatum, and also pontine and medullary nuclei, the cerebellum, and the intermediolateral columns of the spinal cord.[5,6] Nearly all cases to date have been sporadic.

Ideally, one would wish to directly image the aggregated α-Syn load in the synucleinopathies, but this has proved problematic. Given this, imaging studies have relied on demonstrating the structural and functional changes associated with α-Syn pathology.

MRI is able to examine water proton relaxation and the amplitude and direction of water diffusion along nerve fibers enabling alterations in structural connectivity to be detected. It can also detect nigral and striatal iron deposition and loss of nigral melanin as altered susceptibility. Using blood-oxygen-level–dependent (BOLD) sequences, MRI can monitor the slow oscillatory changes in venular oxygenation in brain regions at rest and during actions. Detection of synchronized oscillations of venous oxygenation in different brain regions at rest provides evidence of their functional connectivity, and independent attentional,

*Correspondence to: Dr. David Brooks, Institute of Clinical Medicine, Aarhus University, 44 Nørrebrogade, Aarhus 8000, Denmark; E-mail: AQ4 dbrooks@clin.au.dk

AQ5 **Relevant conflicts of interest/financial disclosures**: Nothing to report. Full financial disclosures and author roles may be found in the online version of this article.

Received: 1 December 2015; **Revised:** 18 December 2015; **Accepted:** 20 December 2015

Published online 00 Month 2016 in Wiley Online Library (wileyonlinelibrary.com). DOI: 10.1002/mds.26547

J_ID: MDS Customer A_ID: MDS26547 Cadmus Art: MDS26547 Ed. Ref. No.: 15-1381.R1 Date: 12-January-16 Stage: Page: 2

executive, visual, motor, and default mode networks have been identified with independent component analysis. The connectivity of these networks becomes disrupted in PD with and without dementia and in MSA.

In the synucleinopathies, radiotracer-based molecular imaging approaches, such as PET and single-photon emission computed tomography (SPECT) can measure in vivo brain metabolism and blood flow and detect changes in their normal patterns of regional covariance. In addition, these modalities are able to detect dysfunction of dopaminergic, noradrenergic, serotonergic, and cholinergic neurotransmission and the abnormal aggregation of beta-amyloid and tau.

Structural Imaging

MRI has been widely used to study changes in structure of the SN, striatum, brainstem, and cerebellum in parkinsonian syndromes. Additionally, tractography has detected early WM damage and loss of structural connectivity.

Substantia Nigra

For a long time, the width of SNc, visualized with T2-weighted sequences (T2W), was the only available structural biomarker of PD.[7] PD patients show lower SNc width, proportional to their level of motor impairment, and a lower mean signal intensity in the SNc.[8] However, T2W MRI failed to detect significant SNc volume changes in early-stage PD. Delineation of SNc was improved by using proton density-weighted and short T1 inversion recovery (STIR) sequences. On STIR images, the SNc is depicted as a well-marginated area of gray matter (GM) signal intensity.

Increased iron deposition can be detected in brain nuclei using sequences sensitive to local magnetic field inhomogeneities, such as T2 and T2*. Compared to controls, patients with PD show decreased relaxation times (T2, T2*) and increased relaxation rates (R2, R2*) in the SNc, putamen, and globus pallidus (GP).[9] Higher R2* in the SNc and red nucleus (RN) correlates with higher UPDRS scores.[10,11] Over a 3-year follow-up, a significant correlation between ΔR2* in the SNc and ΔUPDRS was reported.[12] High R2* signal was reported to be associated with dyskinesias when found in the SNc and RN.[13] However, a second series did not detect such a relationship.[14]

Field-dependent R2 increases (FDRIs) are the differences in measures of tissue R2 obtained with two different field strengths (e.g., 1.5T and 0.5T) and reflect the total iron contained in ferritin molecules. Early-onset (under 60 years) PD patients showed a higher FDRI in the SNc, SNr, putamen, and GP than age-matched controls, which decreases with disease duration,[15] suggesting that dysregulation of iron metabolism occurs in PD.

Recently, relaxation measurements using adiabatic pulse sequences sensitive to molecular motion, known as T1ρ and T2ρ, have highlighted enhanced sensitivity of the T2ρ relaxation measurements when compared to conventional T2. A significant difference between SNc T2ρ values was obtained in PD patients. Moreover, PD patients showed an asymmetry of left and right T1ρ and T2ρ in the SNc, which was not observed in controls.[16]

Susceptibility-weighted imaging (SWI) utilizes R2′ measurements (R2′=R2*-R2, where R2* refers to the actual observed relaxation rate, and R2 refers to the relaxation rate intrinsic to the tissue) to accurately depict brain iron deposition. Lower levels of phase radians in the SNc as well as in the caudate nuclei and RN, with higher phase shift in SNc and basal ganglia (BG), were found in PD patients, implying an increased iron content correlating with UPDRS scores.[17,18] A heterogeneous iron content was noted across PD patients, despite the homogeneity of their unilateral bradykinesia, and rigidity.[19] The combination of SWI and R2* has shown enhanced relaxation and susceptibility in the SNc and anterior GP in PD with R2*, but not SWI, values correlating with tremor and disease duration.[20]

Nigrosomes are small clusters of dopaminergic cells within the SN exhibiting calbindin D28K negativity on immunohistochemical staining. Nigrosome-1 is located in the posterior third of the SNc and returns a high signal on SWI. The healthy nigrosome-1 appearance as a "swallow tail" on 3T-SWI, which is lost in PD.[21] Nigrosome-1 appears as a hyperintense ovoid area within the dorsolateral border of the otherwise hypointense SNc on T2W*, and this also disappears in PD patients.[22] PD patients also show undulations of the smooth lateral SNc surface adjacent to the crus cerebri. These aspects predominated in the more severely affected hemisphere and were not present in healthy subjects.[23]

Diffusion tensor imaging (DTI) allows the tracking of white-matter pathways by measuring the fractional anisotropic (FA) diffusion of water molecules along neuronal axon fibers. In fact, FA is a parameter that relates to the presence of oriented structures, such as axons, in fiber bundles and its reduction may be correlated to fiber degeneration. DTI detects a lower FA of water in the SNc of PD patients, reflecting a loss of directional flow. The greatest FA reduction was observed in the ventrolateral rostral SNc.[24,25] An FA decrease has also been reported in subcortical WM in the supplementary motor area and postcentral somatosensory cortex, a possible explanation for PD-related sensory dysfunction, such as pain, restless legs, akathisia, paresthesia, and dysesthesia.[25,26] However, DTI

ID: pachiyappanm Time: 14:08 I Path: //chenas03/Cenpro/ApplicationFiles/Journals/Wiley/MDS#/Vol00000/150358/Comp/APPFile/JW-MDS#150358

J_ID: MDS Customer A_ID: MDS26547 Cadmus Art: MDS26547 Ed. Ref. No.: 15-1381.R1 Date: 12-January-16 Stage: Page: 3

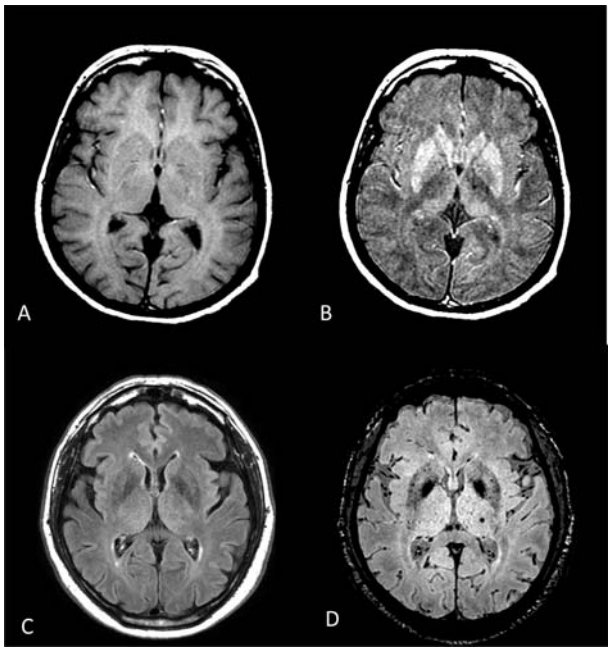

FIG. 1. Comparison of axial MR images passing through the basal ganglia: (A) T1-weighted; (B) T1-weighted with magnetization transfer; (C) FLAIR; and (D) susceptibility-weighted image obtained in 2 parkinsonian patients.

analysis of the whole SNc, as opposed to subregions, failed to discriminate PD patients from controls,[24] despite their higher SN volumes.[27,28] Recently, a positive correlation between baseline free-water values in the posterior SN and subsequent changes in bradykinesia and Montreal Cognitive Assessment scores over 1 year was reported.[29]

Magnetization transfer imaging (MTI) is a nuclear MR technique based on the exchange of magnetization between highly mobile protons and immobile restricted protons on macromolecules, such as myelin or membrane lipids. MTI is able to indirectly image a restricted hydrogen pool, bound to the macromolecules, and has been used in different neurodegenerative disorders. A lower magnetization transfer ratio (MTR) in the SNc in PD was found.[30] This finding was present even in early PD cases.[31] The SNc MTR values did not differ between early and advanced PD patients and did not correlate with UPDRS scores,[32,33] although one series has suggested a correspondence between MTR changes in the SN bilaterally and H & Y/UPDRS scores.[34]

Differential Findings Across Synucleinopathies

On conventional MRI, MSA with predominant parkinsonian symptoms (MSA-P) exhibits putaminal atrophy, T2W hypointensity, and "slit-like" marginal hyperintensities,[35] whereas MSA with predominant cerebellar symptoms (MSA-C) shows atrophy of the lower brainstem, pons, middle cerebellar peduncles, vermis, with pontine cruciform T2W hyperintensity.[36] Pontocerebellar abnormalities are marked in MSA, helping to distinguish this disorder from PD, but not from PSP.[37] Dorsolateral putamen loss of signal in T2* and gradient echo sequences has a high specificity (>0.91) for MSA, though the sensitivity is low unless combined with the presence of a hyperintense lateral rim in fluid-attenuated inversion recovery (FLAIR) sequences (0.97).[38]

MTI can also discriminate parkinsonian syndromes (Fig. 1). Lower MTR values in the GP and SN help F1 separate PD patients from those suffering from PSP and MSA.[33,39,40] MSA patients with pyramidal tract signs have a lower MTR of the corticospinal tract compared to controls and MSA patients without pyramidal signs.[41] Using DTI, MTI, and R2*, the most accurate distinction between MSA, PD, and controls was obtained with putamen bilateral R2* imaging (sensitivity, 77.8%; specificity, 100%).[39]

SWI improves the sensitivity for detecting early MSA from 25% to 75% while preserving a high specificity (91%) by detecting early nigral abnormalities.[42] SWI values of the putamen and pulvinar, showing lower iron deposition, may also help in differentiating MSA-P from PD.[43] Red nucleus hypointensity discriminates PSP from MSA-P and PD, whereas putaminal hypointensity separates PSP and MSA from PD. However, no single or combination of regions of interest are able to accurately discriminate PSP and MSA.[44]

DWI has been widely investigated in parkinsonian syndromes. Greater putaminal regional apparent diffusion coefficient (rADC) has been reported in patients with MSA-P and PSP compared to PD and controls.[45,46] A putamen rADC of 0.760×10^{-3} mm^2/sec discriminated atypical parkinsonism from PD with 96% sensitivity and a 100% positive predictive value. Higher rADC values in caudate, middle cerebral peduncle (MCP), and dorsal putamen (DP) were found in MSA-P compared to PD and controls.[47,48] In particular, MCP rADC values distinguished MSA-P from PD with 92% sensitivity and 100% specificity, more accurately than DP rADC measurements (66.67% sensitivity; 80% specificity). Putaminal trace DWI increases correlated with MSA-P progression and with UPDRS scores,[49] whereas rADC values of MCP positively correlated with age at examination of MSA-P patients.[47]

DTI reveals lower FA and higher mean diffusivity (MD) in the MCP of MSA cases, whereas diffusivity is increased in the decussation of the superior cerebellar peduncles in PSP.[50] Combining tract-based spatial statistics and region of interest (ROI) analyses, a significant reduction of FA values and an increased MD in the bilateral corticospinal tract (CST) and left anterior thalamic radiation (ATR) has also been reported in

ID: pachiyappanm Time: 14:08 I Path: //chenas03/Cenpro/ApplicationFiles/Journals/Wiley/MDS#/Vol00000/150358/Comp/APPFile/JW-MDS#150358

COLOR

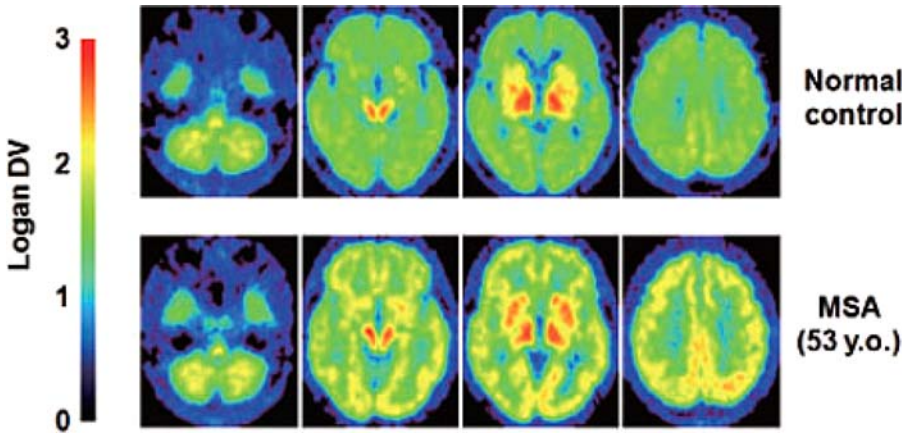

FIG. 2. ^{11}C-BF227 PET in a normal subject and a case of probable MSA. The MSA case increased cortical, basal ganglia, and white matter signal reflecting α-Syn aggregates.[60] DV, distribution volume.

MSA-P patients.[51] There was a correlation between disease duration and FA values in the left CST and between UPDRS motor score and FA values in the right CST. Findings of regional DTI analysis reveal specific differences among parkinsonisms. Compared to PD, MSA-P cases show lower FA in the body of corpus callosum (CC), anterior corona radiate, CST, middle and inferior cerebellar peduncles, medial lemniscus, and posterior limb of the internal capsule bilaterally. Compared to MSA, PSP cases show higher MD in the ATR and superior cerebellar peduncle.[52]

In advanced clinical stages of MSA, atrophy of the pons, cerebellum, and middle cerebellar peduncles becomes evident.[53] Atrophy of the pontocerebellar system results in the T2W "hot-cross bun" sign.[54] In MSA, MRI can detect a reduction of anteroposterior diameter of the midbrain, pons, and fourth ventricle, with atrophy of the cerebellum, bulbar olive, and midbrain.[41] MSA-C may be suspected when brainstem volumetric decrease occurs in parallel with cerebellar atrophy.[55]

DTI of nondemented PD (PDND) cases has shown a lower FA in frontal, temporal, and occipital WM (OWM) compared to controls. A lower FA in bilateral posterior cingulate projections distinguished PDD from PDND patients correlating with cognitive and attentional performance in PD.[56]

Impaired cognitive performance has also been associated with increased MD of central WM tracts. Specifically, increased MD in frontal and parietal tracts was associated with poor performances on semantic fluency and the executive Tower of London tasks.[57] Central white matter degeneration occurs early in PD, and its presence could predict susceptibility to later cognitive dysfunction.

Executive dysfunction has been correlated to DTI variations in the frontal projection fibers, the genu of corpo callosum, and in the superior fronto-occipital fasciculus.[58] Short-term memory alterations have been associated with DTI changes in the fornix, whereas long-term memory deficit have been paired to DTI abnormalities in the right anterior corona radiate. Attention domain dysfunction has been mapped with DTI to diffusion changes in left cingulate gyrus and the splenium, whereas language impairment was associated with DTI changes in the frontal connecting WM regions.

Functional Imaging

Imaging α-Syn

Whereas a number of small molecules bind in vivo to aggregated α-Syn, a selective imaging biomarker has, to date, proved elusive. First, α-Syn aggregates exist in multiple forms, only some of which may be toxic to cells. In PD, the bulk of α-Syn exists in oligomeric, rather than fibrillar, form, in contrast to beta-amyloid (Aβ) in Alzheimer's disease (AD), which is mainly in a fibrillar state. Peptides and antibodies that bind selectively to these α-Syn aggregates do not readily cross the blood–brain barrier (BBB) when administered intavenously. Because PET (^{11}C, 20 minutes; ^{18}F, 110 minutes) and SPECT (^{123}I, 13 hours) isotopes have only short half-lives, peptides and antibodies radiolabeled with these nuclei do not make suitable in vivo brain imaging agents. A number of small polyaromatic molecules have now been identified that cross the BBB and bind to α-Syn fibrils. Unfortunately, these molecules, such as BF227,[59] also tend to bind to other aggregated proteins if present, including Aβ plaques. They are also lipophilic, and so radiotracers based on these structures yield significant nonspecific background signals. Other examples of such molecules include 1-{6-[(2-[^{18}F]Fluoroethyl)(methyl)amino]-2-naphthyl} ethylidene)malononitrile, and the diphenylpyrazole derivative, Anle138. ^{11}C-BF227 PET has been used to measure the aggregated α-Syn load in 8 cases with probable MSA (see Fig. 2).[60] Mean signal F2
was increased by around 15% in central WM and the

ID: pachiyappanm Time: 14:08 I Path: //chenas03/Cenpro/ApplicationFiles/Journals/Wiley/MDS#/Vol00000/150358/Comp/APPFile/JW-MDS#150358

BG of the MSA cases, though the individual ranges overlapped with those of healthy controls.

Pittsburgh compound B (PiB) is a neutral phenothiazole that binds to both Aβ and α-Syn fibrils in vitro. However, ^{11}C-PiB uptake in vivo was normal in 2 MSA cases studied.[61] Whereas ^{11}C-BF227 PET does not have the sensitivity or specificity to diagnose MSA, it could, in principle, still be used to monitor changes in α-Syn aggregant load after interventions such as immunotherapy. Levels of other aggregated proteins, such as Aβ, would first have to be independently determined. In practice, given that in vivo determinations of α-Syn aggregant load with imaging are problematic, functional MRI (fMRI), PET, or SPECT are currently used to study its effects on brain function.

The Dopaminergic System

Dopamine terminal function in the synucleinopathies, PD, DLB, and MSA, can be examined in vivo with both PET and SPECT[62]: (1) The availability of presynaptic dopamine transporters (DATs) to ligands has been assessed with PET and SPECT tropane-based radiotracers, such as ^{18}F-CFT, ^{123}I-FP-CIT (DaTscan), ^{18}F-FP-CIT, ^{123}I-beta-CIT, ^{123}I-altropane, and ^{99m}Tc-TRODAT, and also nontropane ligands, such as ^{11}C-methylphenidate and ^{11}C-nomifensine. (2) The activity of aromatic acid decarboxylase (AADC), the enzyme that converts levodopa to dopamine, has been measured with ^{18}F-dopa PET. (c) Vesicle monoamine transporter binding in dopamine terminals can be detected with PET using the dihydrotetrabenazines, ^{11}C-DTBZ or ^{18}F-DTBZ (AV-133).

Early hemiparkinsonian cases with late-onset idiopathic PD show bilaterally reduced putamen dopaminergic function targeting the posterior subregion, activity being more depressed in the putamen contralateral to the affected limbs. Dopaminergic function in the head of caudate and ventral striatum is relatively spared. This is also the case for genetic PD associated with LRRK2[63] and GBA mutations.[64] PET and SPECT are also able to detect subclinical disease in H & Y stage 1 late-onset genetic and sporadic PD cases, evidenced as involvement of the "asymptomatic" putamen contralateral to the clinically unaffected limbs.[65,66] It has been estimated that clinical parkinsonism occurs when PD patients have lost around 50% of their posterior putamen dopamine terminal function.[67]

^{11}C-methylphendiate PET detected significant reductions in putamen DAT binding in two of three asymptomatic carriers of the LRRK2 gene where ^{18}F-dopa PET was normal, suggesting that DAT loss provides a more sensitive marker of early terminal dysfunction than ADDC loss.[63] However, ^{18}F-dopa PET has also detected subclinical disease in both asymptomatic adult LRRK2[68] and in GBA[64] cases. Additionally, ^{18}F-dopa PET can demonstrate adaptive changes to putamen dopamine terminal dysfunction, detecting internal pallidal rises in AADC activity in early PD, which later fall as the disease progresses.[69] Forty elderly relatives of PD patients who had no overt parkinsonism, but who manifested idiopathic hyposmia on olfactory screening, have been investigated with baseline beta-CIT SPECT and then followed clinically. Seven of these forty relatives showed reduced ^{123}I-beta-CIT uptake in one or more striatal subregions, and the 4 with lowest DAT binding subsequently converted to clinical PD over a 2-year follow-up period.[70]

In DLB, putamen dopaminergic loss is more symmetrical than in PD and there is a greater involvement of the head of caudate. Imaging-pathological correlations have shown that FP-CIT SPECT can successfully separate DLB from AD in life because dopaminergic function remains intact in the latter.[71] MSA cases show a similar asymmetric loss of putamen function to idiopathic PD, but the head of caudate tends to be more involved. Having said this, it has not proved possible to reliably discriminate between PD and MSA by imaging their pattern of loss of presynaptic dopaminergic function.[72,73]

In series where clinically probable parkinsonian and essential tremor cases have been compared, imaging the dopamine system with PET and SPECT has been shown to differentiate these conditions with a sensitivity and specificity greater than 90%.[74,75] Given this, an abnormal PET or SPECT scan should be valuable for supporting a diagnosis of dopamine deficient parkinsonism where there is diagnostic doubt. What still remains uncertain is whether the finding of normal dopaminergic function with PET or SPECT fully excludes a diagnosis of PD. The majority of patients clinically thought to have PD, but with normal ^{18}F-dopa PET or DAT SPECT imaging, so-called subjects without evidence of dopamine deficiency (SWEDDs), generally show little clinical progression or change in dopamine imaging findings on long-term follow-up.[76,77] The majority of SWEDDs are later reclassified as having a benign or dystonic tremor, whereas other diagnoses included small vessel disease and drug-induced syndromes. Having said that, occasional SWEDDs in the Parkinson's Progression Markers Iniative series have been observed 2 years down the line to develop reduced striatal FP-CIT uptake (J. Seibyl, personal communication). These cases, however, all had baseline DAT imaging at the low end of normal. In general, a finding of normal presynaptic dopaminergic function on imaging is associated with a good prognosis in a case of suspected PD whatever the ultimate diagnosis.

Putamen dopamine D2 receptor availability may be measured with benzamides, such as ^{11}C-raclopride

PET or ^{123}I-iodobenzamide (IBZM) SPECT, and can rise in early untreated PD because dopamine deficiency makes more receptors available to radioligands.[78] This rise in D2 binding normalizes after chronic exposure to L-dopa.[79] In contrast, MSA is associated with loss of putamen dopamine D2 binding resulting from degeneration of the nucleus.[80,81] This reduction, however, is mild and so does not provide a sensitive discriminator of MSA from PD. In one series, ^{123}I-IBZM SPECT detected reduced striatal D2 binding in two thirds of de novo parkinsonian patients who had a negative apomorphine response and were thought to have early MSA.[82]

Following Synucleinopathy Progression

Imaging biomarkers can, in principle, be used to objectively monitor progression of synucleinopathies and, more important, examine the effects of putative neuroprotective and restorative agents on their course. A limitation is that these biomarkers give information about only one aspect of the disease, such as levels of dopaminergic function or glucose metabolism. Additionally, the use of such biomarkers assumes that therapeutic interventions have no direct effects on the imaging itself. This has proved to be problematic in practice because chronic exposure to medication can unexpectedly influence uptake and binding of imaging agents.

Initial studies using ^{18}F-dopa PET and DAT SPECT reported a 5% to 12% annual decline in putamen dopamine terminal function in early PD patients over 2 to 4 years.[67,83] These, initially de novo, PD cases, however, were all exposed to dopamine agonists and L-dopa during the course of these series. More recently, a similar, slower rate of decline has been reported for agonist alone or placebo-treated cases.[84] These findings suggest that exposure to L-dopa, though not dopamine agonists, may accelerate a reduction in DAT binding per se. If this is the case, studies determining rate of loss of dopamine terminal function using ^{18}F-dopa PET and DAT SPECT as biomarkers of efficacy of potentially neuroprotective drugs may be confounded if L-dopa is a concommitant treatment.

To date, neuroprotective studies using imaging biomarkers have been negative. The c-Jun N-terminal kinase inhibitor, CEP1347, the vitamin, coenzyme Q10, that promotes mitochondrial aerobic respiration, the neuroimmunophylline GPI1845, and the glutamate release inhibitor, riluzole, have all failed to influence disease progression either clinically or with imaging measures in PD. Interestingly, CEP1347 had an unsuspected depressant effect on striatal beta-CIT uptake.[84]

Loss of striatal D2 binding can be used to follow MSA progression. IBZM SPECT has been reported to detect an annual 10% loss of putamen D2 availability in one MSA series.

^{18}F-2-fluoro-2-deoxyglucose (FDG) is taken up by brain regions, phosphorylated by hexokinase, and the product, FDG-P, is trapped. Its uptake thus provides a measure of regional cerebral glucose utilization (rCMRGlc), which primarily reflects neuronal synaptic activity. In nondemented PD patients, covariance analysis reveals an abnormal profile of relatively increased lentiform nucleus and reduced frontoparietal metabolism.[85] This has been labeled the PD-related profile (PDRP), and its degree of expression correlates with levels of motor disability rated with the UPDRS. Expression of the PDRP increases with disease progression whereas successful treatment of locomotor symptoms with either dopaminergic replacement therapy or DBS acts to normalize the PDRP.[86-88] ^{18}FDG-PET studies in MSA show reduced levels of striatal, brainstem, and cerebellar glucose metabolism, in contrast to PD where these are preserved.[89,90] Striatal FDG uptake correlates with disability in MSA and so, in principle, can be used to follow progression of MSA by monitoring the loss of striatal glucose metabolism over time.fMRI can also be used to track progression of PD. Using BOLD sequences to monitor synchronization of the slow oscillatory changes in venular oxygenation at rest across brain regions the functional connectivity of attentional, executive, visual, motor, and default mode networks can be identified with independent component analysis. Reduced attentional network connectivity has been shown to correlate with impaired performance of Stroop and Trail Making B tasks in PD, whereas increased default mode connectivity correlated with impaired performance on visual perception tests.[91] This disruption of brain connectivity in PD worsens over time and potentially can be used as a biomarker of disease progression.[92]

Tremor and Serotonergic Dysfunction

Serotonergic cell function can be assessed either by measuring median raphe serotonin HT_{1A} binding of cell bodies in the midbrain or the availability of serotonin transporters (SERT) on terminals in the brainstem and cortex. HT_{1A} sites act as autoreceptors on serotonergic cell bodies in the median raphe, but are also found postsynaptically on pyramidal cells in the limbic cortex. They can be detected with ^{11}C-WAY100635 or ^{18}F-MPPF PET. A 25% loss of median raphe HT_{1A} binding has been reported in PD with ^{11}C-WAY100635 PET, which correlated inversely with severity of rest tremor, though not with levels of rigidity or bradykinesia.[93] Brainstem raphe SERT binding can be measured with ^{11}C-DASB PET,

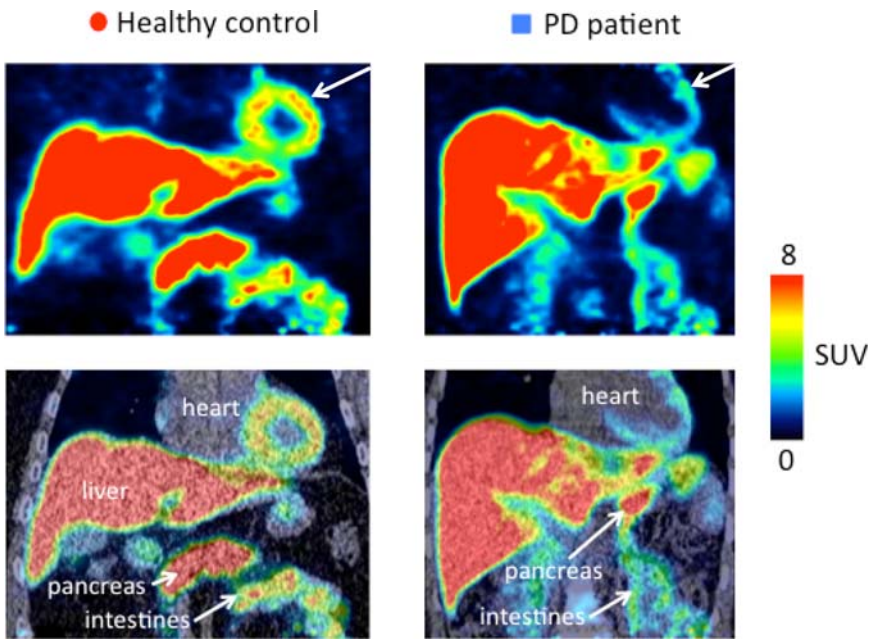

COLOR

FIG. 3. ^{11}C-donepezil PET showing reduced small intestine and pancreas cholinesterase activity in a PD case.[107]

^{123}I-beta CIT, or ^{123} I-FP-CIT SPECT. Decreases in raphe SERT binding have also been reported to correlate with tremor severity and persistence.[94,95] These findings suggest that midbrain tegmentum pathology may be more relevant than nigrostriatal projection loss to the etiology of PD tremor.

Mechanisms of Dementia in Synucleinopathies

Dementia is multifactorial in PD and is associated with the presence of cortical LB disease, concomitant AD and small vessel pathology, and degeneration of dopaminergic and cholinergic projections to cortical regions. LB and AD pathology both target cortical association areas. FDG PET detects impaired glucose utilization in the posterior cingulate, parietal, and temporal association areas, but in PDD and DLB patients, there is significantly greater occipital hypometabolism than in AD.[96] In nondemented PD cases who develop isolated cognitive problems, covariance analysis detects an abnormal cognitive profile, the PD cognition-related pattern (PDCP), which is separate from the PDRP profile associated with locomotor dysfunction.[97] The PDCP is characterized by relative glucose metabolic reductions in medial frontal and parietal association regions and relative increases in cerebellar cortex and dentate nuclei. Its expression in individual subjects correlates with performance on neuropsychological tests of memory and executive functioning.

^{11}C-NMP4A and ^{11}C-PMP PET are markers of acetylcholine esterase activity, so their uptake indirectly reflects cholinergic terminal function. Nondemented PD patients show reduced cholinergic function in parietal and occipital cortex, and levels correlate with performance on tests of attention and learning, though not with locomotor disability.[98] In PDD, cholinergic loss spreads to involve all areas of cortex.[99] Levels of cortical ^{11}C-PMP uptake in PD correlate with Mini–Mental State Examination (MMSE) scores, whereas reduced thalamic cholinergic function is associated with gait and balance disorders. This possibly reflects loss of cholinergic projections from the pedunculo-pontine nucleus to the thalamus.[100] Interestingly, in MSA, cortical cholinergic function is relatively preserved, perhaps explaining the lower prevalence of dementia. Cholinergic function, however, is reduced in the striatum, pons, and cerebellum of MSA cases, possibly contributing to their early postural instability.[101]

^{11}C-PIB PET detects Aβ deposition in a minority of PDD patients, suggesting that amyloid pathology is not the major contributor to their cognitive problems.[102,103] In contrast, a majority of DLB patients, where onset of dementia has coincided with parkinsonism, show increased cortical ^{11}C-PIB signal. DLB is therefore a dual pathology syndrome as currently clinically defined explaining its aggressive nature. Interestingly, nondemented PD patients who have a raised amyloid load on ^{11}C-PIB PET develop cognitive deficits more rapidly when followed than those who are amyloid free at baseline.[104]

Systemic Organ Dysfunction in Synucleinopathies

Iodine-123-metaiodobenzylguanidine (^{123}I-MIBG) SPECT is a marker of adrenergic terminal function

AQ10

TABLE 1. Synopsis of the MRI studies in synucleinopathies

AQ8

Author	Cases	Controls	Field Strenght	Technique	Primary Measure	Findings	Clinical implications
Bartzokis et al., 1999	14 PD	14	1.5T 0.5T	T2	FDRI	FDRI increase in SNc, SNr, putamen, and GP	Early-onset PD patients ↑ of FDRI in the SNc, SNr, putamen, and GP; late-onset patients ↓ FDRI in the SNr
Oikawa et al., 2002	22 PD	22	1.5T	T2 Proton-density STIR	SN size (STIR axis perpendicular to SN)	No significant differences in the size of the SN between PD patients and healthy controls	
Kosta et al., 2004	40 PD	40	1.5T	T2	T2	Higher T2 in the putamen and GP in PD	Lower T2 in the STN in PD with disease duration >5 years
von Lewinski et al., 2006	88 PD 52 MSA	29	1.5T	T2*	Signal Intensity Putamen/ thalamus Putamen/ caudate	Putaminal hypointensity in thalamus or CN in 63.5% of MSA patients, but in only 6.8% of PD and 13.8% of controls	Hyperintense lateral putaminal rim in combination with loss of putaminal signal enhanced the ability in finding MSA patients.
Michaeli et al., 2006	8 PD	8	4.0T	T2w	T1ρ T2ρ	↓T2ρ values in the SN in PD; T2 was not able to show significant differences between PD and controls; T2ρ and T1ρ maps asymmetry in PD vs. controls	
Wallis et al., 2008	65 PD	10	1.5T	T2*	R2*	No significant relationship between disease duration and R2* in the SN, FWM, and putamen	Positive correlation between UPDRS score and SN R2*
Kwon et al., 2012	10 PD	10	7.0T	T2*	Volumetric analysis	↓Area of high signal intensity in SN; increased size of the area of low signal intensity	
Blazejewska et al., 2013	10 PD	8	7.0T	T2*	Signal Intensity	Bilateral absence of hyperintense area in SN	
Lewis et al., 2013	38 PD (26 with dyskinesia)	23	3.0T	T2 T2*	R2*	Higher R2* values in the SN an RN in PD patients compared to controls	PD patients without dyskinesia have a significant higher R2* in the SN, but not in the RN compared to controls; PD patients with dyskinesia have a significant higher R2* both in the SN and RN compared to PD without dyskinesia and controls; positive correlation between UPDRS-III score and R2* in the SN and RN.

(Continued)

ID: pachiyappanm Time: 14:08 I Path: //chenas03/Cenpro/ApplicationFiles/Journals/Wiley/MDS#Vol00000/150358/Comp/APPFile/JW-MDS#150358

J_ID: MDS Customer A_ID: MDS26547 Cadmus Art: MDS26547 Ed. Ref. No.: 15-1381.R1 Date: 12-January-16 Stage: Page: 8

TABLE 1. *Continued*

AQ8 Author	Cases	Controls	Field Strenght	Technique	Primary Measure	Findings	Clinical implications
Aquino et al., 2013	42 PD (22 EPD 20 LPD)	20	1.5T	T2* DTI	Volume R2* FA MD	The only obtained significant difference between PD patients and healthy controls is for SN area and volume.	SN area differed between late PD and early PD and between early PD and controls and between late PD and controls, whereas SN volume differences are significant only between late PD and early PD/controls.
Wieler et al., 2014	19 PD	13	3.0T	T2*	R2*	In contrast to the baseline findings, results over a 36-month follow-up do not show a significant difference in measured R2* in the SNc between PD and controls.	Correlation between R2* changes over 36 months and disease severity
Ulla et al., 2014	27 PD	26	1.5T	T2*	R2*	Increased R2* of the SN in PD patients	Positive correlation between ΔR2* and ΔUPDRS over a 3-year follow-up
Gupta et al., 2009	11 PD 12 MSA 12 PSP	11	1.5T	SWI	Hypointensity score (HS)	↑HS in RN in parkinsonisms; ↑putamen HS in PSP vs. PD, but no difference between PSP and MSA-P or between PSP and PD; ↑SN HS in PSP in comparison to MSA-P and PD	
Zhang et al., 2009	42 PD	30	1.5T	SWI	Phase shift values (PV)	↓PV in SNc, CN, and RN in PD patients	Positive correlation between UPDRS and SN in the most affected side in PD patients
Zhang et al., 2010	40 PD	20	3.0T	SWI	Phase shift values (PV)	↑PV in the most affected side in PD patients than in control subjects	PS correlate with UPDRS score
Wang et al., 2011	21 PD 10 MSA	54	1.5T	SWI	Phase shift values (PV)	↑Iron deposition in the SN of PD and MSA-P patients compared to healthy controls	No difference between PD and MSA-P in iron deposition in SN, but higher deposition in putamen and posterior thalami in MSA-P compared to PD
Rossi et al., 2013	37 PD	21	3.0T	T2w T2* SWI	R2* SWI	↑Relaxation and susceptibility effects in the SN and anterior GP in PD patients compared to controls	Disease duration correlates with R2* in the medial SN; no significant correlation between SWI signal and clinical characteristics.

(Continued)

ID: pachiyappanm Time: 14:08 I Path: //chenas03/Cenpro/ApplicationFiles/Journals/Wiley/MDS#Vol00000/150358/Comp/APPFile/JW-MDS#150358

J_ID: MDS Customer A_ID: MDS26547 Cadmus Art: MDS26547 Ed. Ref. No.: 15-1381.R1 Date: 12-January-16 Stage: Page: 9

TABLE 1. *Continued*

Author	Cases	Controls	Field Strenght	Technique	Primary Measure	Findings	Clinical implications
Schwarz et al., 2014	8 PD	8	3.0T	SWI	Signal intensity	Loss of hyperintensity area in SN ("swallow tail")	
Rossi et al., 2014	32 PD	19	3.0T	T2 SWI T2* DTI		↑ Iron-related relaxation in GP, CN, and SN	↑ Iron related: in anterior GP associated with MCI; in CN associated with later onset; in the SNc over 2-year follow-up
Dashtipour et al., 2015	12 PD		3.0T	SWI	Phase shift values (PV)		Heterogeneity of brain iron accumulation in PD
Reiter et al., 2015	104 PD 22 MSA 22 PSP	42	3.0T	SWI	Signal Intensity	Absence of dorsolateral nigral hyperintensity in all the groups of patients	SWI not able to distinguish PD from other parkinsonian syndromes
Meijer et al., 2015	38 PD 12 MSA 3 PSP	13	3.0T	SWI	Signal Intensity	Severe hypointensity of the putamen in MSA-P	No changes in susceptibility of the SN or other brain structures in PD in comparison to atypical parkinsonism or controls
Hutchinson and Raff, 2000	6 PD		1.5T	IR		Lateral thinning and low signal in early-stage PD, especially in the upper section of SNc; late-stage PD patients show low signal also in the medial segment of SNc (loss of signal in a lateral-to-medial gradient in SNc)	High correlation between radiological index and UPDRS score
Atasoy et al., 2004	20 PD	16	1,5T	T2w	VIS	Lower SNc intensity and width, lower putamen volumes in PD patients compared to controls	Presence of correlation between SNc intensity score and UPDRS score
Seppi et al., 2003	13 PD 12 MSA 10 PSP		1.5T	DWI	rADC	Higher rADC values in the putamen and in the CN in MSA-P and PSP compared to PD patients	No differences between MSA-P and PSP groups
Seppi et al., 2005	10 PD 10 MSA		1.5T	DWI	Trace (D)	Greater increase of Trace(D) in the putamen in MSA-P patients compared to PD patients	↑ Trace(D) in the putamen and correlation with UPDRS-III score
Schocke et al., 2003	17 PD 10 MSA	10	1.5T	DWI	rADC	Higher rTrace and rADC in y direction in MSA-P compared to PD and controls	DWI parameters correlate with UPDRS-III score
Blain et al., 2006	12 PD 17 MSA 17 PSP	12	1.5T	DTI	FA MD	↓FA and ↓MD in MDC in MSA vs. PSP, PD and controls and in DSCP in PSP vs. PD (MD also vs. MSA)	FA and MD abnormalities able to distinguish between MSA and PSP

(Continued)

ID: pachiyappanm Time: 14:08 I Path: //chenas03/Cenpro/ApplicationFiles/Journals/Wiley/MDS#Vol00000/150358/Comp/APPFile/JW-MDS#150358

J_ID: MDS Customer A_ID: MDS26547 Cadmus Art: MDS26547 Ed. Ref. No.: 15-1381.R1 Date: 12-January-16 Stage: Page: 10

TABLE 1. *Continued*

AQ8 Author	Cases	Controls	Field Strenght	Technique	Primary Measure	Findings	Clinical implications
Nicoletti et al., 2006	16 PD 16 MSA 16 PSP	15	1.5T	DWI	rADC	↑ rADC in putamen in MSA patients vs. PSP, PD, and controls; ↑ rADC in CN in MSA compared to PD, but not PSP; ↑ rADC in putamen in PSP compared to PD and controls; ↑ rADC in the MCP in MSA compared to PSP, PD, and controls	Correlation between rADC values in the MCP and age at examination (but not with other clinical characteristics, including age at onset, disease duration, H & Y scale, and UPDRS score)
Beyer et al., 2005	35 PD (19 PDND + 16 PDD)	20	1.5T	T2w	WMH	↑ WMH in deep WM and periventricular areas in PDD compared to PDND	Significant correlation between WMH and MMSE score
Beyer et al., 2007	36 PD (20 PDND + 16 PDD)	20	1.5T	VBM	Volume	GM ↓ in frontal, parietal, limbic, and temporal lobes in PDD compared to PDND and in the right superior temporal gyrus compared to controls	↓GM in specific cortical areas correlates with cognitive impairment in PD patients.
Vaillancourt et al., 2009	14 PD	14	3.0T	DTI	FA	↓ FA in the SN of PD vs. controls	FA of specific ROI is able to discriminate PD from controls.
Menke at al., 2009	10 PD	10	3.0T	DTI	Volume FA	↓ Volumes of the whole SN in PD vs. controls (but not significant)	No discrimination with FA↓ in the SN between PD and controls
Zhan et al., 2012	12 PD	20	4.0T	DTI	FA	↓ FA not only in the SN, but also in the WM closer to cortical regions involved in motor controls and somatosensory cortex	Regional FA ↓ correlates with UPDRS score.
Zhang et al., 2015	27 PD	50	3.0T	DTI	FA	↓ FA of the nigrostriatal tract in PD patients regardless of the side of motor symptom onset	Significant relationship between DTI alterations and UPDRS-III score
Chung et al., 2009	12 PD 10 MSA	10	1.5T	DWI	rADC	↑rADC values of the dorsal putamen and MCP in MSA-P vs. PD	rADC values do not correlate with clinical features in either MSA or PD.

(Continued)

ID: pachiyappanm Time: 14:08 I Path: //chenas03/Cenpro/ApplicationFiles/Journals/Wiley/MDS#/Vol00000/150358/Comp/APPFile/JW-MDS#150358

J_ID: MDS Customer A_ID: MDS26547 Cadmus Art: MDS26547 Ed. Ref. No.: 15-1381.R1 Date: 12-January-16 Stage: Page: 11

TABLE 1. *Continued*

Author	Cases	Controls	Field Strenght	Technique	Primary Measure	Findings	Clinical implications
Worker et al., 2014	14 PD 16 MSA 16 PSP	17	1.5T	DTI	FA MD	PSP vs. PD: ↓ FA in PSP in the CC, CR, CST, ATR, SCP, EC, retrolenticular, and ALIC bilaterally; MSA vs. PD: ↓FA in the CC, CR, CST, MCP and ICP, ML, and PLIC bilaterally in MSA; PSP vs. MSA:↑ MD in PSP group in the anterior thalamic radiation and SCP; PD vs. MSA or PSP: No region showed reduced FA or decreased MD.	Significant relationship between DTI alterations (FA and MD) and H & Y scale of severity disease
Wang et al., 2015	20 PD 15 MSA	20	3.0T	DTI	FA rD	↓ FA and higher RD of the bilateral CST and left ATR in MSA-P vs. PD	Significant correlation between disease duration and FA values in the left CST as well as left ATR, and between UPDRS motor score and FA values in the right CST
Ofori et al., 2015	25 PD	19	3.0T	DTI	Free-water values FA	↑Free water in the posterior SN and ↑FA in the anterior SN in PD after 1-year follow-up	Correlation between baseline free-water values in the posterior SN and change in bradykinesia over 1 year
Matsui et al., 2007	37 PD (26 PDND + 11 PDD)	10	1.5T	DTI	FA	↓FA in PD in FWM, TWM, and OWM; ↓FA in PDD compared to PDND in bilateral posterior CG	FA values in the left posterior CG correlated with many cognitive parameters, whereas FA values in the right CG correlated with attention.
Zheng et al., 2014	16 PD	/	3.0T	DTI	FA MD	DTI changes depend on cognitive parameters: *executive dysfunctions*: frontal regions, CC, SFO, and sagittal striatum; *short-term memory*: fornix; *long-term memory*: right anterior CR; *attention*: left cingulate gyrus and splenium; *language*: FWM	Correlation between DTI changes and cognitive impairment
Duncan et al., 2015	125 PD	50	3.0T	DTI	Volume FA MD	in PD patients, ↑in the MD of central WM in the absence of ↓in either FA or GM volume	↑MD in frontal-parietal tracts and ↓GM volume in frontal, parietal, and temporal areas correlated with poor performance on the semantic fluency and executive Tower of London tasks

(Continued)

TABLE 1. *Continued*

AQ8 Author	Cases	Controls	Field Strenght	Technique	Primary Measure	Findings	Clinical implications
Hanyu et al., 2001	17 PD (11 PDND + 6 PDD) 6 PSP	12	1.5T	MTI	MTR	↓MTR in subcortical WM (FWM and genu of the CC) in PDD vs. PD or controls; ↓MTR in subcortical WM and in GM in PSP compared to PD and controls	No differences in MTR between PD patients and controls; MTR variations between PDD and PD
Naka et al., 2002	12 MSA (7 MSA-C + 5 MSA-P)	11	1.5T	MTI	MTR	↓MTR in the precentral gyrus WM, posterior limb of the internal capsule, MCP, and pons in MSA with pyramidal tract signs vs. MSA without pyramidal tract signs and controls	Differences in MTR values in MSA, especially in those present pyramidal signs
Tambasco et al., 2003	11 PD	8	3.0T	MTI	MTR	↓MTR in SNc, red nucleus, pons, WM, and brainstem in PD vs. controls	MTR of specific ROIs individuates PD vs. controls
Eckert at al., 2003	15 PD 12 MSA 19 PSP	20	1.5T	MTI	MTR	↓MTR of the GP in PSP patients; ↓MTR in the putamen in MSA vs. PD and controls; ↓MTR in the SN in PSP, MSA, and PD	↓MTR in specific ROIs points to parkinsonisms.
Anik et al., 2007	33 PD	30	1.5T	MTI	MTR	↓MTR in the SNc, SNr, RN, and pons in PD compared to controls	Evidence of ↓ MTR values in early PD
Tambasco et al., 2011	22 PD	10	3.0T	MTI	MTR	↓MTR in PD patients in the SNc, SNr, putamen, and parietal WM compared to controls	↓MTR extends to caudate, FWM, and pons with disease course; no correlation between MTR and age at or UPDRS score.
Morgen at al., 2011	36 PD	23	1.5T	MTI	MTR	↓MTR in bilateral SN and left olfactory cortex bordering on the amygdala	Correlation between MTR and H & Y stage and UPDRS score
Focke et al., 2011	12 PD 10 MSA 9 PSP	13	3.0T	MTI T2* DWI	MTR R2*, R2, R1-mapping MD, FA	↑MTR in the left CN in PD patients compared to controls; ↑R2* in the putamen bilaterally and right GP in MSA-P vs. controls; ↓MTR in the putamen bilaterally and left SN in MSA-P compared to PD; ↑MD in the GP and SN bilaterally in PSP compared to controls; ↑MTR in the right GP in PSP compared to PD	R2* mapping separates patients with MSA from those with PD.

(Continued)

ID: pachiyappanm Time: 14:08 I Path: //chenas03/Cenpro/ApplicationFiles/Journals/Wiley/MDS#Vol00000/150358/Comp/APPFile/JW-MDS#150358

J_ID: MDS Customer A_ID: MDS26547 Cadmus Art: MDS26547 Ed. Ref. No.: 15-1381.R1 Date: 12-January-16 Stage: Page: 13

TABLE 1. *Continued*

Author	Cases	Controls	Field Strenght	Technique	Primary Measure	Findings	Clinical implications
Bunzeck et al., 2013	20 PD	20	3.0T	MTI T2*	Volume, MTR R2*	↓Volume and MTR in the SN in PD compared to controls	Positive correlation between R2* and tremulous motor symptoms in the putamen, CN, and thalamus

ALIC, anterior limb of the internal capsula; CD, caudate nucleus; CG, cingulated bundle; CR, corona radiate; DSCP, decussation of superior cerebellar peduncles; EC, external capsula; FWM, frontal white matter; ICP, inferior cerebellar peduncle; IR, inversion recovery; MCI, mild cognitive impairment; MDC, middle cerebellar peduncles; ML, medial lemniscus; PLIC, posterior limb of the internal capsula; SCP, superior cerebellar peduncle; SFO, superior fronto-occipital fasciculus; TWM, temporal white matter; VBM, voxel-based morphometry; VIS, Volume Intensity Score; WMH, white matter hyperintensity.

AQ8

and can be used to study functional integrity of cardiac sympathetic innervation in PD. Myocardial/mediastinal ^{123}I-MIBG signal ratios are reduced in over 80% of PD cases, even when cardiac autonomic reflexes are intact.[105] ^{123}I-MIBG SPECT is normal in most MSA patients as the autonomic dysfunction arises from loss of pre- rather than postsynaptic sympathetic innervation.[106]

^{11}C-donepezil PET is a marker of acetylcholine esterase (AChE) activity in brain and systemic organs. In PD cases, the small intestine and pancreas show a significant reduction in ^{11}C-donepezil standardized uptake value (SUV; Fig. 3).[107] Myocardial AchE activity in myocardium is also mildly reduced. Loss of systemic ^{11}C-donepezil uptake could reflect reduced vagal cholinergic innervation given that the dorsal nucleus of the vagus is targeted by LB pathology. However, the myenteric plexus also contains AChE, and local pathology could also contribute to the signal loss. F3

Conclusions

The differential diagnosis of synucleinopathies represents a challenge. Currently, no neuroimaging has the power to diagnose PD or atypical parkinsonism, but its findings can be highly supportive of differential diagnoses and help highlight the differences among the parkinsonisms. Though we are currently unable to selectively image aggregates of α-Syn, their structural and functional consequences can be detected. Detection of dopamine deficiency in synucleinopathies rationalizes trials of dopaminergic medication where diagnostic doubt exists. Detection of reduced striatal dopaminergic function in gene carriers at risk for PD will allow identification of cases for neuroprotective trials. Both MRI and radiotracer-based imaging provide potential biomarkers for following progression of synucleinopathies and assessing the efficacy of putative neuroprotective and restorative approaches. However, direct effects of interventions on imaging modalities have proven to be a confound in the interpretation of past trials, and these need to be excluded when designing future studies.

Functional imaging has helped to understand the mechanisms underlying nonmotor complications of PD, including dementia and depression, and can rationalize nondopaminergic therapeutic approaches. ■

References

1. Braak H, Ghebremedhin E, Rub U, Bratzke H, Del Tredici K. Stages in the development of Parkinson's disease-related pathology. Cell Tissue Res 2004;318:121-134.
2. Hely MA, Reid WG, Adena MA, Halliday GM, Morris JG. The Sydney multicenter study of Parkinson's disease: the inevitability of dementia at 20 years. Mov Disord 2008;23:837-844.
3. McKeith IG, Galasko D, Kosaka K, et al. Consensus guidelines for the clinical and pathologic diagnosis of dementia with Lewy

bodies (DLB): report of the Consortium on DLB International Workshop. Neurology 1996;47:1113-1124.

4. Armstrong RA, Cairns NJ, Lantos PL. Beta-amyloid deposition in the temporal lobe of patients with dementia with Lewy bodies: comparison with non-demented cases and Alzheimer's disease. Dement Geriatr Cogn Disord 2000;11:187-192.
5. Gilman S, Wenning GK, Low PA, et al. Second consensus statement on the diagnosis of multiple system atrophy. Neurology 2008;71:670-676.
6. Wenning GK, Jellinger KA. The role of alpha-synuclein in the pathogenesis of multiple system atrophy. Acta Neuropathol (Berl) 2005;109:129-140.
7. Savoiardo M, Girotti F, Strada L, Ciceri E. Magnetic resonance imaging in progressive supranuclear palsy and other parkinsonian disorders. J Neural Transm Suppl 1994;42:93-110.
8. Pujol J, Junque C, Vendrell P, Grau JM, Capdevila A. Reduction of the substantia nigra width and motor decline in aging and Parkinson's disease. Arch Neurol 1992;49:1119-1122.
9. Kosta P, Argyropoulou MI, Markoula S, Konitsiotis S. MRI evaluation of the basal ganglia size and iron content in patients with Parkinson's disease. J Neurol 2006;253:26-32.
10. Wallis LI, Paley MN, Graham JM, et al. MRI assessment of basal ganglia iron deposition in Parkinson's disease. J Magn Reson Imaging 2008;28:1061-1067.
11. Lewis MM, Du G, Kidacki M, et al. Higher iron in the red nucleus marks Parkinson's dyskinesia. Neurobiol Aging 2013;34: 1497-1503.
12. Ulla M, Bonny JM, Ouchchane L, Rieu I, Claise B, Durif F. Is R2* a new MRI biomarker for the progression of Parkinson's disease?. A longitudinal follow-up. PLoS One 2013;8:e57904.
13. Bunzeck N, Singh-Curry V, Eckart C, et al. Motor phenotype and magnetic resonance measures of basal ganglia iron levels in Parkinson's disease. Parkinsonism Relat Disord 2013;19:1136-1142.
14. Wieler M, Gee M, Martin WR. Longitudinal midbrain changes in early Parkinson's disease: iron content estimated from R2*/MRI. Parkinsonism Relat Disord 2015;21:179-183.
15. Bartzokis G, Cummings JL, Markham CH, et al. MRI evaluation of brain iron in earlier- and later-onset Parkinson's disease and normal subjects. Magn Reson Imaging 1999;17:213-222.
16. Michaeli S, Oz G, Sorce DJ, et al. Assessment of brain iron and neuronal integrity in patients with Parkinson's disease using novel MRI contrasts. Mov Disord 2007;22:334-340.
17. Zhang W, Sun SG, Jiang YH, Qiao X, Sun X, Wu Y. Determination of brain iron content in patients with Parkinson's disease using magnetic susceptibility imaging. Neurosci Bull 2009;25: 353-360.
18. Zhang J, Zhang Y, Wang J, et al. Characterizing iron deposition in Parkinson's disease using susceptibility-weighted imaging: an in vivo MR study. Brain Res 2010;1330:124-130.
19. Dashtipour K, Liu M, Kani C, et al. Iron accumulation is not homogenous among patients with Parkinson's disease. Parkinsons Dis 2015;2015:324843.
20. Rossi M, Ruottinen H, Soimakallio S, Elovaara I, Dastidar P. Clinical MRI for iron detection in Parkinson's disease. Clin Imaging 2013;37:631-636.
21. Schwarz ST, Afzal M, Morgan PS, Bajaj N, Gowland PA, Auer DP. The 'swallow tail' appearance of the healthy nigrosome—a new accurate test of Parkinson's disease: a case-control and retrospective cross-sectional MRI study at 3T. PLoS One 2014;9: e93814.
22. Blazejewska AI, Schwarz ST, Pitiot A, et al. Visualization of nigrosome 1 and its loss in PD: pathoanatomical correlation and in vivo 7 T MRI. Neurology 2013;81:534-540.
23. Kwon DH, Kim JM, Oh SH, et al. Seven-Tesla magnetic resonance images of the substantia nigra in Parkinson disease. Ann Neurol 2012;71:267-277.
24. Vaillancourt DE, Spraker MB, Prodoehl J, et al. High-resolution diffusion tensor imaging in the substantia nigra of de novo Parkinson disease. Neurology 2009;72:1378-1384.
25. Zhang Y, Wu IW, Buckley S, et al. Diffusion tensor imaging of the nigrostriatal fibers in Parkinson's disease. Mov Disord 2015; 30:1229-1236.
26. Zhan W, Kang GA, Glass GA, et al. Regional alterations of brain microstructure in Parkinson's disease using diffusion tensor imaging. Mov Disord 2012;27:90-97.
27. Menke RA, Scholz J, Miller KL, et al. MRI characteristics of the substantia nigra in Parkinson's disease: a combined quantitative T1 and DTI study. Neuroimage 2009;47:435-441.
28. Aquino D, Contarino V, Albanese A, et al. Substantia nigra in Parkinson's disease: a multimodal MRI comparison between early and advanced stages of the disease. Neurol Sci 2014;35:753-758.
29. Ofori E, Pasternak O, Planetta PJ, et al. Increased free water in the substantia nigra of Parkinson's disease: a single-site and multi-site study. Neurobiol Aging 2015;36:1097-1104.
30. Tambasco N, Pelliccioli GP, Chiarini P, et al. Magnetization transfer changes of grey and white matter in Parkinson's disease. Neuroradiology 2003;45:224-230.
31. Anik Y, Iseri P, Demirci A, Komsuoglu S, Inan N. Magnetization transfer ratio in early period of Parkinson disease. Acad Radiol 2007;14:189-192.
32. Tambasco N, Belcastro V, Sarchielli P, et al. A magnetization transfer study of mild and advanced Parkinson's disease. Eur J Neurol 2011;18:471-477.
33. Tambasco N, Nigro P, Romoli M, Simoni S, Parnetti L, Calabresi P. Magnetization transfer MRI in dementia disorders, Huntington's disease and parkinsonism. J Neurol Sci 2015;353:1-8.
34. Morgen K, Sammer G, Weber L, et al. Structural brain abnormalities in patients with Parkinson disease: a comparative voxel-based analysis using T1-weighted MR imaging and magnetization transfer imaging. AJNR Am J Neuroradiol 2011;32:2080-2086.
35. Konagaya M, Sakai M, Matsuoka Y, Goto Y, Yoshida M, Hashizume Y. Pathological correlate of the slitlike changes on MRI at the putaminal margin in multiple system atrophy. J Neurol 1999;246:142-143.
36. Schrag A, Kingsley D, Phatouros C, et al. Clinical usefulness of magnetic resonance imaging in multiple system atrophy. J Neurol Neurosurg Psychiatry 1998;65:65-71.
37. Yekhlef F, Ballan G, Macia F, Delmer O, Sourgen C, Tison F. Routine MRI for the differential diagnosis of Parkinson's disease, MSA, PSP, and CBD. J Neural Transm 2003;110:151-169.
38. von Lewinski F, Werner C, Jorn T, Mohr A, Sixel-Doring F, Trenkwalder C. T2*-weighted MRI in diagnosis of multiple system atrophy. A practical approach for clinicians. J Neurol 2007; 254:1184-1188.
39. Focke NK, Helms G, Pantel PM, et al. Differentiation of typical and atypical Parkinson syndromes by quantitative MR imaging. AJNR Am J Neuroradiol 2011;32:2087-2092.
40. Eckert T, Sailer M, Kaufmann J, et al. Differentiation of idiopathic Parkinson's disease, multiple system atrophy, progressive supranuclear palsy, and healthy controls using magnetization transfer imaging. Neuroimage 2004;21:229-235.
41. Naka H, Imon Y, Ohshita T, et al. Magnetization transfer measurements of brain structures in patients with multiple system atrophy. Neuroimage 2002;17:1572-1578.
42. Reiter E, Mueller C, Pinter B, et al. Dorsolateral nigral hyperintensity on 3.0T susceptibility-weighted imaging in neurodegenerative parkinsonism. Mov Disord 2015;30:1068-1076.
43. Wang Y, Butros SR, Shuai X, et al. Different iron-deposition patterns of multiple system atrophy with predominant parkinsonism and idiopathetic Parkinson diseases demonstrated by phase-corrected susceptibility-weighted imaging. AJNR Am J Neuroradiol 2012;33:266-273.
44. Gupta D, Saini J, Kesavadas C, Sarma PS, Kishore A. Utility of susceptibility-weighted MRI in differentiating Parkinson's disease and atypical parkinsonism. Neuroradiology 2010;52:1087-1094.
45. Seppi K, Schocke MF, Esterhammer R, et al. Diffusion-weighted imaging discriminates progressive supranuclear palsy from PD, but not from the parkinson variant of multiple system atrophy. Neurology 2003;60:922-927.
46. Schocke MF, Seppi K, Esterhammer R, et al. Diffusion-weighted MRI differentiates the Parkinson variant of multiple system atrophy from PD. Neurology 2002;58:575-580.
47. Nicoletti G, Lodi R, Condino F, et al. Apparent diffusion coefficient measurements of the middle cerebellar peduncle differentiate the Parkinson variant of MSA from Parkinson's disease and progressive supranuclear palsy. Brain 2006;129(Pt 10):2679-2687.

J_ID: MDS Customer A_ID: MDS26547 Cadmus Art: MDS26547 Ed. Ref. No.: 15-1381.R1 Date: 12-January-16 Stage: Page: 16

48. Chung EJ, Kim EG, Bae JS, et al. Usefulness of diffusion-weighted MRI for differentiation between Parkinson's disease and Parkinson variant of multiple system atrophy. J Mov Disord 2009;2:64-68.
49. Seppi K, Schocke MF. An update on conventional and advanced magnetic resonance imaging techniques in the differential diagnosis of neurodegenerative parkinsonism. Curr Opin Neurol 2005; 18:370-375.
50. Blain CR, Barker GJ, Jarosz JM, et al. Measuring brain stem and cerebellar damage in parkinsonian syndromes using diffusion tensor MRI. Neurology 2006;67:2199-2205.
51. Ji L, Wang Y, Zhu D, Liu W, Shi J. White matter differences between multiple system atrophy (parkinsonian type) and Parkinson's disease: a diffusion tensor image study. Neuroscience 2015; 305:109-116.
52. Worker A, Blain C, Jarosz J, et al. Diffusion tensor imaging of Parkinson's disease, multiple system atrophy and progressive supranuclear palsy: a tract-based spatial statistics study. PLoS One 2014;9:e112638.
53. Savoiardo M, Strada L, Girotti F, et al. Olivipontocerebellar atrophy: MR diagnosis and relationship to multisystem atrophy. Radiology 1990;174:693-696.
54. Konayaga M, Konayaga Y, Iida M. Clinical and magnetic resonance imaging study of extrapyramidal symptoms in multiple system atrophy. J Neurol Neurosurg Psychiatry 1994;57:1528-1531.
55. Schulz JB, Skalej M, Wedekind D, et al. Magnetic resonance imaging-based volumetry differentiates idiopathic Parkinson's syndrome from multiple system atrophy and progressive supranuclear palsy. Ann Neurol 1999;45:65-74.
56. Matsui H, Nishinaka K, Oda M, Niikawa H, Kubori T, Udaka F. Dementia in Parkinson's disease: diffusion tensor imaging. Acta Neurol Scand 2007;116:177-181.
57. Duncan GW, Firbank MJ, Yarnall AJ, et al. Gray and white matter imaging: a biomarker for cognitive impairment in early Parkinson's disease? Mov Disord 2015 Jul 22. doi: 10.1002/mds.26312. [Epub ahead of print]
58. Zheng Z, Shemmassian S, Wijekoon C, Kim W, Bookheimer SY, Pouratian N. DTI correlates of distinct cognitive impairments in Parkinson's disease. Hum Brain Mapp 2014;35:1325-1333.
59. Fodero-Tavoletti MT, Mulligan RS, Okamura N, et al. In vitro characterisation of BF227 binding to alpha-synuclein/Lewy bodies. Eur J Pharmacol 2009;617:54-58.
60. Kikuchi A, Takeda A, Okamura N, et al. In vivo visualization of alpha-synuclein deposition by carbon-11-labelled 2-[2-(2-dimethylaminothiazol-5-yl)ethenyl]-6-[2-(fluoro)ethoxy]benzoxazole positron emission tomography in multiple system atrophy. Brain 2010;133(Pt 6):1772-1778.
61. Claassen DO, Lowe VJ, Peller PJ, Petersen RC, Josephs KA. Amyloid and glucose imaging in dementia with Lewy bodies and multiple systems atrophy. Parkinsonism Relat Disord 2011;17:160-165.
62. Brooks DJ, Frey KA, Marek KL, et al. Assessment of neuroimaging techniques as biomarkers of the progression of Parkinson's disease. Exp Neurol 2003;184(Suppl 1):S68-S79.
63. Adams JR, van Netten H, Schulzer M, et al. PET in LRRK2 mutations: comparison to sporadic Parkinson's disease and evidence for presymptomatic compensation. Brain 2005;128(Pt 12): 2777-2785.
64. Goker-Alpan O, Masdeu JC, Kohn PD, et al. The neurobiology of glucocerebrosidase-associated parkinsonism: a positron emission tomography study of dopamine synthesis and regional cerebral blood flow. Brain 2012;135(Pt 8):2440-2448.
65. Morrish PK, Sawle GV, Brooks DJ. Clinical and [18F]dopa PET findings in early Parkinson's disease. J Neurol Neurosurg Psychiatry 1995;59:597-600.
66. Marek K, Seibyl JP, Zoghbi SS, et al. [I-123] beta-CIT SPECT imaging demonstrates bilateral loss of dopamine transporters in hemiparkinsons disease. Neurology 1996;46:231-237.
67. Morrish PK, Rakshi JS, Sawle GV, Brooks DJ. Measuring the rate of progression and estimating the preclinical period of Parkinson's disease with [18F]dopa PET. J Neurol Neurosurg Psychiatry 1998;64:314-319.
68. Nicholl DJ, Vaughan JR, Khan NL, et al. Two large British kindreds with familial Parkinson's disease: a clinico-pathological and genetic study. Brain 2002;125(Pt 1):44-57.
69. Whone AL, Moore RY, Piccini P, Brooks DJ. Plasticity in the nigropallidal pathway in Parkinson's disease: an 18F-dopa PET study. Ann Neurol 2003;53:206-213.
70. Ponsen MM, Stoffers D, Booij J, Van Eck-Smit BL, Wolters E, Berendse HW. Idiopathic hyposmia as a preclinical sign of Parkinson's disease. Ann Neurol 2004;56:173-181.
71. Walker Z, Jaros E, Walker RW, et al. Dementia with lewy bodies: a comparison of clinical diagnosis, FP-CIT SPECT imaging and autopsy. J Neurol Neurosurg Psychiatry 2007;78:1176-1181.
72. Burn DJ, Sawle GV, Brooks DJ. The differential diagnosis of Parkinson's disease, multiple system atrophy, and Steele-Richardson-Olszewski syndrome: discriminant analysis of striatal 18F-dopa PET data. J Neurol Neurosurg Psychiatry 1994;57:278-284.
73. Pirker W, Asenbaum S, Bencsits G, et al. [I-123]beta-CIT SPECT in multiple system atrophy, progressive supranuclear palsy, and corticobasal degeneration. Mov Disord 2000;15:1158-1167.
74. Brooks DJ, Playford ED, Ibanez V, et al. Isolated tremor and disruption of the nigrostriatal dopaminergic system: an 18F-dopa PET study. Neurology 1992;42:1554-1560.
75. Benamer TS, Patterson J, Grosset DG, et al. Accurate differentiation of parkinsonism and essential tremor using visual assessment of [123I]-FP-CIT imaging: The [123I]-FP-CIT Study Group. Mov Disord 2000;15:503-510.
76. Marshall VL, Patterson J, Hadley DM, Grosset KA, Grosset DG. Two-year follow-up in 150 consecutive cases with normal dopamine transporter imaging. Nucl Med Commun 2006;27:933-937.
77. Marek K, Seibyl J, Eberly S, et al. Longitudinal follow-up of SWEDD subjects in the PRECEPT Study. Neurology 2014;82: 1791-1797.
78. Antonini A, Schwarz J, Oertel WH, Beer HF, Madeja UD, Leenders KL. [11C]raclopride and positron emission tomography in previously untreated patients with Parkinson's disease: influence of L-dopa and lisuride therapy on striatal dopamine D2-receptors. Neurology 1994;44:1325-1329.
79. Turjanski N, Lees AJ, Brooks DJ. PET studies on striatal dopaminergic receptor binding in drug naive and L-dopa treated Parkinson's disease patients with and without dyskinesia. Neurology 1997;49:717-723.
80. Pavese N, Simpson BS, Metta V, Ramlackhansingh A, Chaudhuri KR, Brooks DJ. [(1)(8)F]FDOPA uptake in the raphe nuclei complex reflects serotonin transporter availability. A combined [(1)(8)F]FDOPA and [(1)(1)C]DASB PET study in Parkinson's disease. Neuroimage 2012;59:1080-1084.
81. Brooks DJ, Ibanez V, Sawle GV, et al. Striatal D2 receptor status in Parkinson's disease, striatonigral degeneration, and progressive supranuclear palsy, measured with 11C-raclopride and PET. Ann Neurol 1992;31:184-192.
82. Schwarz J, Tatsch K, Gasser T, et al. 123I-IBZM binding compared with long-term clinical follow up in patients with de novo parkinsonism. Mov Disord 1998;13:16-19.
83. Marek K, Innis R, van Dyck C, et al. [123I]beta-CIT SPECT imaging assessment of the rate of Parkinson's disease progression. Neurology 2001;57:2089-2094.
84. Parkinson, Group S. Mixed lineage kinase inhibitor CEP-1347 fails to delay disability in early Parkinson disease. Neurology 2007;69:1480-1490.
85. Eidelberg D, Moeller JR, Dhawan V, et al. The metabolic anatomy of Parkinson's disease: complementary [18F]fluorodeoxyglucose and [18F]fluorodopa positron emission tomographic studies. Mov Disord 1990;5:203-213.
86. Feigin A, Fukuda M, Dhawan V, et al. Metabolic correlates of levodopa response in Parkinson's disease. Neurology 2001;57: 2083-2088.
87. Lin TP, Carbon M, Tang C, et al. Metabolic correlates of subthalamic nucleus activity in Parkinson's disease. Brain 2008;131(Pt 5):1373-1380.
88. Hilker R, Voges J, Weisenbach S, et al. Subthalamic nucleus stimulation restores glucose metabolism in associative and limbic cortices and in cerebellum: evidence from a FDG-PET study in advanced Parkinson's disease. J Cereb Blood Flow Metab 2004; 24:7-16.
89. Antonini A, Kazumata K, Feigin A, et al. Differential diagnosis of parkinsonism with [18F]fluorodeoxyglucose and PET. Mov Disord 1998;13:268-274.

ID: pachiyappanm Time: 14:08 I Path: //chenas03/Cenpro/ApplicationFiles/Journals/Wiley/MDS#/Vol00000/150358/Comp/APPFile/JW-MDS#150358

90. Spetsieris PG, Ma Y, Dhawan V, Eidelberg D. Differential diagnosis of parkinsonian syndromes using PCA-based functional imaging features. Neuroimage 2009;45:1241-1252.

91. Baggio HC, Segura B, Sala-Llonch R, et al. Cognitive impairment and resting-state network connectivity in Parkinson's disease. Hum Brain Mapp 2015;36:199-212.

92. Olde Dubbelink KT, Schoonheim MM, Deijen JB, Twisk JW, Barkhof F, Berendse HW. Functional connectivity and cognitive decline over 3 years in Parkinson disease. Neurology 2014;83:2046-2053.

93. Doder M, Rabiner EA, Turjanski N, Lees AJ, Brooks DJ. Tremor in Parkinson's disease and serotonergic dysfunction: an (11)C-WAY 100635 PET study. Neurology 2003;60:601-605.

94. Loane C, Wu K, Bain P, Brooks DJ, Piccini P, Politis M. Serotonergic loss in motor circuitries correlates with severity of action-postural tremor in PD. Neurology 2013;80:1850-1855.

95. Qamhawi Z, Towey D, Shah B, et al. Clinical correlates of raphe serotonergic dysfunction in early Parkinson's disease. Brain 2015; 138(Pt 10):2964-2973.

96. Minoshima S, Foster NL, Sima AA, Frey KA, Albin RL, Kuhl DE. Alzheimer's disease versus dementia with Lewy bodies: cerebral metabolic distinction with autopsy confirmation. Ann Neurol 2001;50:358-365.

97. Huang C, Mattis P, Perrine K, Brown N, Dhawan V, Eidelberg D. Metabolic abnormalities associated with mild cognitive impairment in Parkinson disease. Neurology 2008;70(16 Pt 2):1470-1477.

98. Bohnen NI, Kaufer DI, Hendrickson R, et al. Cognitive correlates of cortical cholinergic denervation in Parkinson's disease and parkinsonian dementia. J Neurol 2006;253:242-247.

99. Hilker R, Thomas AV, Klein JC, et al. Dementia in Parkinson disease: functional imaging of cholinergic and dopaminergic pathways. Neurology 2005;65:1716-1722.

100. Bohnen NI, Albin RL. The cholinergic system and Parkinson disease. Behav Brain Res 2011;221:564-573.

101. Gilman S, Koeppe RA, Nan B, et al. Cerebral cortical and subcortical cholinergic deficits in parkinsonian syndromes. Neurology 2010;74:1416-1423.

102. Edison P, Rowe CC, Rinne J, et al. Amyloid load in Lewy body dementia (LBD), Parkinson's disease dementia (PDD) and Parkinson's disease (PD) measured with C-11-PIB PET. Neurology 2007;68:A98-A98.

103. Gomperts SN, Rentz DM, Moran E, et al. Imaging amyloid deposition in Lewy body diseases. Neurology 2008;71:903-910.

104. Gomperts SN, Locascio JJ, Rentz D, et al. Amyloid is linked to cognitive decline in patients with Parkinson disease without dementia. Neurology 2013;80:85-91.

105. Nagayama H, Hamamoto M, Ueda M, Nagashima J, Katayama Y. Reliability of MIBG myocardial scintigraphy in the diagnosis of Parkinson's disease. J Neurol Neurosurg Psychiatry 2005;76: 249-251.

106. Druschky A, Hilz MJ, Platsch G, et al. Differentiation of Parkinson's disease and multiple system atrophy in early disease stages by means of I-123-MIBG-SPECT. J Neurol Sci 2000;175: 3-12.

107. Gjerloff T, Fedorova T, Knudsen K, et al. Imaging acetylcholinesterase density in peripheral organs in Parkinson's disease with 11C-donepezil PET. Brain 2015;138(Pt 3):653-663.

SGML and CITI Use Only
DO NOT PRINT

Author Roles

(1) Research Project: A. Conception, B. Organization, C. Execution; (2) Statistical Analysis: A. Design, B. Execution, C. Review and Critique; (3) Manuscript Preparation: A. Writing of the First Draft, B. Review and Critique.

Financial Disclosures

Nothing to report.

AQ1: A short running title within the journal limit of 50 characters has been added. Please approve as OK.

AQ2: Please provide degrees for each author.

AQ3: Please confirm or correct author affiliations; Please also provide departmental names for affiliations 2 and 3.

AQ4: Please confirm that "Dr." is correct honorific for corresponding author. Please also confirm that all details for contact information are appearing completely and correctly.

AQ5: All financial disclosure or conflicts of interest related to the research in this article must be listed, regardless of time frame. Please confirm that these are appearing completely and correctly.

AQ6: All articles with more than one author must provide a list of author roles based on, but not necessarily limited to, the template as shown. Please include a complete list of roles for each author.

AQ7: All financial disclosure for the past 12 months regardless of relationship to this research for each author must be listed. Please confirm that this information is appearing completely and correctly. See "Instructions to Authors" for details.

AQ8: For left column of Table 1, please include corresponding reference numbers after year, for instance, "Author et al., year[xx]".

AQ9: Please confirm that given names (red) and surnames/family names (green) have been identified correctly.

AQ10: Please check whether Table 1 is OK as typeset.